ASSESSMENT OF THE DYNAMIC BEHAVIOR OF MONOLITHIC PRESTRESSED CONCRETE HIGHWAY VIADUCTS

Wael A. Zatar, PhD, Associate Professor, College of Information Technology and Engineering, Marshall University, Huntington, WV

ABSTRACT

The aspect of clarifying the inelastic response of prestressed concrete (hereafter PC) highway viaducts during severe earthquakes recently gained a considerable importance. An on-going research effort to clarify the dynamic response of PC highway viaducts is carried out. Experimental and analytical investigations were conducted utilizing scaled models of highway viaducts. Specimens representing PC girders of the viaducts were examined using two experimental techniques. A sub-structuring technique was implemented in such a way that the response of the PC girder was revealed experimentally, and the responses of RC columns of the highway viaduct model were simulated simultaneously. Response analyses for the viaduct model were carried out. The accuracy of the analytical model was evaluated through comparing the experimental and analytical results. The study revealed that not only the RC columns but also the PC girders of PC viaducts may undergo considerable damage during earthquakes. A parametric study that was aimed at identifying the significant parameters that influence the dynamic behavior of PC highway viaducts was carried out. Recommendations pertaining to the seismic behavior and design of monolithic PC highway viaducts are proposed.

KEYWORDS: Prestressed Concrete, Earthquake Resistant Structures, Viaduct Structures, Sub-Structured Pseudo-Dynamic Testing, Statically Reversed Cyclic Loading Tests, Dynamic Analysis.

INTRODUCTION

Viaduct structures and bridges are becoming a logical choice for railways and highways. Prestressed concrete has been used for the construction of viaduct structures during the past few decades. Earthquakes identify structural weakness and concentrating the damage at these locations. Bridges and viaduct structures have little or no redundancy in structural systems and failure of one structural element or connection is thus more likely to result in collapse [1]. Many experimental investigations have been carried out in the past to study the deformation and cracking of partially prestressed concrete beams under static and cyclic fatigue loading [2]. Various loading tests have been carried out to study the inelastic response behavior of the bridges when subjected to ground motions. Since the girders of these bridges are generally supported on the columns or bridge bents, only the columns are subjected to earthquake forces. Moreover, few research studies have been carried out to study the effect of prestressing the reinforced concrete columns of highway bridges [3], [4]. Therefore, it is of a great importance to carefully understand the seismic response behavior of monolithic highway viaduct structures.

Because of the monolithic moment-resisting connection between the superstructure and the columns of the viaduct structures, less bending moments are expected in the bottom ends of the columns and other plastic hinges at the tip of the columns may result to allow for some energy dissipation at these locations. Moreover, not only the columns but also the girders might have some damage. Not enough tests have been performed yet to study the inelastic response behavior of the partially prestressed concrete (hereafter known as PC) girders of the viaduct structures [5], [6], and [7]. The objective of this study is to obtain the inelastic response behavior of such PC viaduct structures due to severe earthquake excitations.

A study, which included experimental and analytical phases, was carried out. Specimens representing the PC girders of the viaduct structures were tested experimentally. Statically reversed cyclic loading and sub-structured pseudo-dynamic testing schemes are employed. The objective of the statically reversed cyclic loading test was to study the inelastic response behavior of the PC girders and to obtain the hysteretic-load deformational characteristics. During the sub-structured pseudo-dynamic test, the PC girder was tested experimentally and the RC columns of the viaduct structure were simulated analytically. Response analyses for the viaduct model in terms of hysteretic moment-rotation curves and time-histories were carried out. The plastic deformability expressed in terms of the ductility factor and the dissipated energy was examined. A comparison between the experimental results and results obtained from response analyses is made in this study.

OUTLINES OF EXPERIMENTAL INVISTIGATION

TEST SPECIMENS

The viaduct model (Fig. 1) was constructed at a 1/10 scale of a full size viaduct structure. The PC girder of the viaduct structure was considered as the experimental substructure. It

was reasonably assumed that the viaduct girder was symmetric with respect to the center of each bay. This assumption was made for simplicity and due to the difficulty of implementing members with different inflection points, and because of the linearly varying moment distribution. Consequently, the PC girder was assumed to be composed of two identical cantilever members satisfying compatibility and equilibrium conditions at the center. Only half of the PC girder was considered as the experimental member (Fig. 1a). The model numbering scheme, dimensions, and degrees of freedom are shown in Fig. 1b.

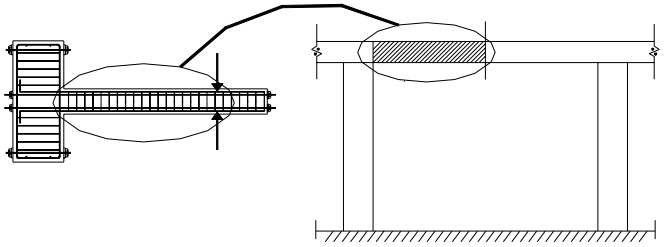

a) Experimental test specimen

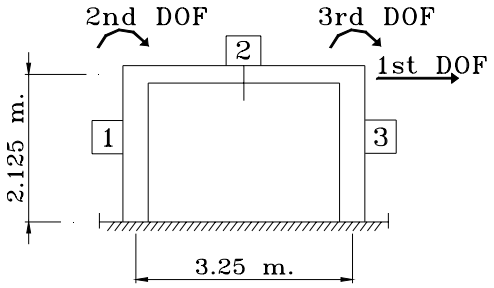

b) Model used in the sub-structured pseudo-dynamic testing

Fig. 1 Experimental Test Specimen and Model used in The Sub-Structured Pseudo-Dynamic Testing

Two partially PC specimens representing the experimental PC girder members of the viaduct models and named B-1 and B-2 were tested. The specimens have the same dimensions, reinforcing bars and prestressing tendons arrangement. Specimen B-1 was tested using a statically reversed cyclically loading while specimen B-2 was tested using a sub-structured pseudo-dynamic test. The upper part of each specimen (Fig. 2) represents the PC girder part. The PC girder part was placed monolithically with a lower part. The lower part represents the moment resisting connection and the upper part of the reinforced concrete column of the viaduct model. The lower part has sufficient rigidity to allow the observation of the damage of the PC girders during testing.

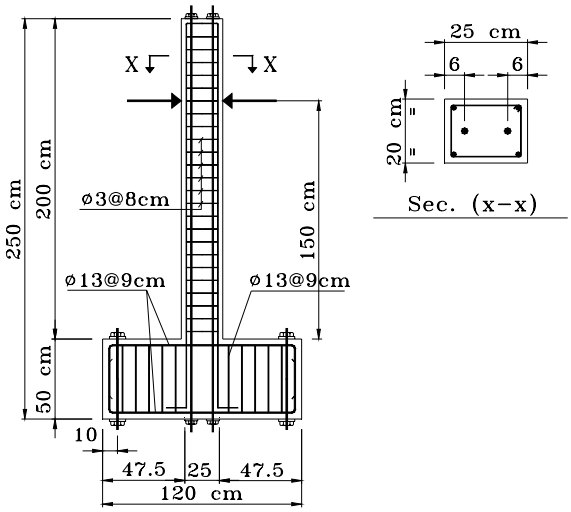

a) Test specimens

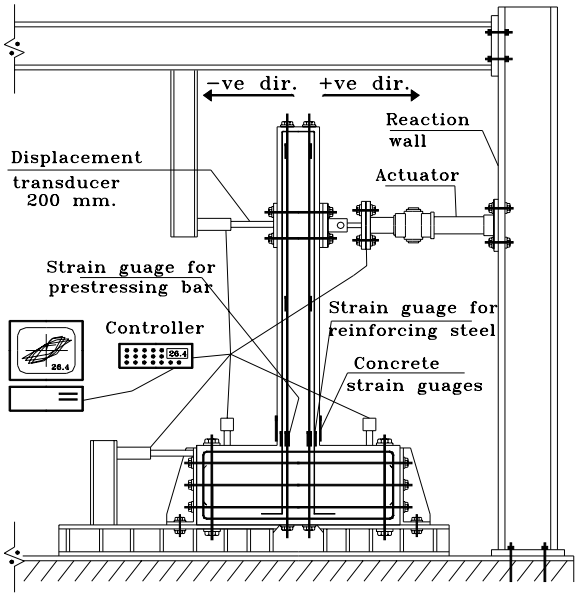

b) Loading setup

Fig. 2 Test Specimens and Loading Setup

The PC girder part has a depth of 25 cm, a width of 20 cm, and a length of 200 cm. The lower part of the specimen has a depth of 50 cm, a width of 50 cm, and a length of 120 cm. The girder part has two reinforcing bars with 13 mm diameter at each side of the section. The girder part has one D11 mm prestressing tendon at each side of the cross section (Fig. 2). The mechanical prestressing ratio of the specimens is 0.55. The design philosophy implicitly requires that shear failure be prevented or delayed so that the member under consideration may dissipate, by flexure, energy larger than required for the applied earthquake. Therefore,

relatively close-spaced transverse hoops were arranged for the entire length of the girder part. The rectangular hoops were 3 mm in diameter and were spaced at 80 mm.

The specimens were fixed to a testing floor by the use of side supports, prestressed rods, and high strength bolts. The loading was applied through an actuator that was fixed at a height of 150 cm from the bottom end of the PC girder of each specimen (Fig. 2). The corresponding *a/d* ratio is 6.8. The average compressive cylindrical concrete strength is 400 kgf/cm^2. The yield strength of the reinforcing bars is 3400 kgf/cm^2 and the yield strength of the prestressing tendons is 12200 kgf/cm^2. Details of the specimens are shown in Fig. 2.

STATICALLY REVERSED CYCLIC LOADING TESTING

Statically reversed cyclic loading test was carried out for specimen B-1. The objective of conducting this test was to clarify the load-displacement characteristics of the PC girders. The specimen was tested using the setup shown in Fig. 2b. The setup consisted of the specimen, actuator, reaction wall, testing floor, data loggers, computer for data acquisition, and displacement measuring devices. The yield displacement was the measured displacement corresponding to the recorded yield load. The imposed displacements to the specimen through the actuator were multiples of the prestressing tendons yielding displacement. Ten repetitions of each cycle were considered. Typically, ten repetitions cannot be attained during a real severe earthquake but they were planned to fully clarify the load-displacement characteristics. Fig. 3 shows the input displacements that were applied to specimen B-1.

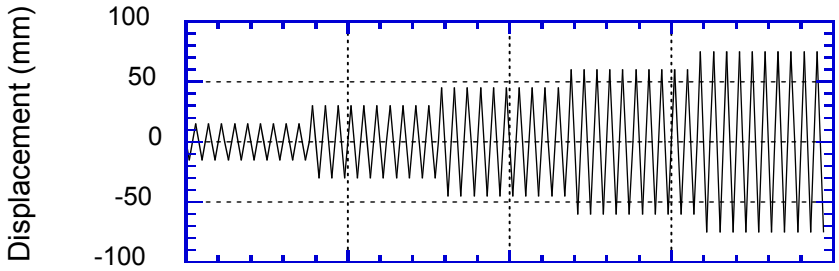

Fig. 3 Input Displacements to Specimen B-1 in the Statically Reversed Cyclic Loading Test

SUB-STRUCTURED PSEUDO-DYNAMIC TESTING

Structural Model

Many numerical and experimental studies have been carried out to clarify the inelastic behavior of RC columns. However, very few experimental studies have been carried out to date on the response behavior of the full structures in which few members may undergo extensive inelastic deformations. The inelastic deformations of the few members may significantly affect the overall response behavior and the structure integrity of the full

structure. The unavailability of test records for the full viaduct structures can be attributed to the high cost and scale of conducting the associated large tests.

Sub-structured pseudo-dynamic test is a computer-controlled experimental technique in which direct numerical time integration is used to solve the equation of motion. By incorporating the sub-structuring concept, it is possible to test only the critical member effect on the inelastic seismic response of the whole structure.

The PC girder of the viaduct structure was considered as the experimental sub-structure. The PC girder was assumed to be composed of two identical cantilever members satisfying compatibility and equilibrium conditions at the center, and thus having only half of the girder as the experimental member (Fig. 1a).

Experimental Procedures

The sub-structured pseudo-dynamic testing technique was used for testing specimen B-2 of the viaduct model shown in Fig. 1b. The load was applied quasi-statically during the test and the dynamic effects were simulated numerically [8]. An analytical inelastic mechanical model and its restoring force-displacement model were used for all the RC members of the viaduct structure except for the PC girder [9]. The restoring force for the PC girder was measured directly from the loading test system [10].

One component model [11] was employed for the inelastic member model. The one component model consists of a linearly elastic member with two equivalent non-linear springs at the member ends (Fig. 4a). The rotational deformation of the member due to the bending moment was expressed as the sum of the flexural deformation of the linear elastic member and the rotational deformation of the two equivalent non-linear springs. The spring constants are known as K_{PA} and K_{PB} (Fig. 4a) and are determined using Otani's method [12]. The inelastic moment-rotation relationship of the spring was calculated by means of the ordinary flexural theory based on the assumption that the point of contra flexure was located at the center of each member. Furthermore, the rotations due to bond-slip of the reinforcing bars as well as the prestressing tendons from the connecting joint were taken into consideration using Ohta's method [13] for all the members of the viaduct model.

Takeda's et al. tri-linear model [14] was used as the hysteretic restoring force model for the RC members (Fig. 4b). Takeda's et al. model includes the characteristic behavior of concrete cracking, yielding, and strain hardening of the main reinforcement. Takeda's et al. model is a realistic and conceptual model that recognizes the continually degrading stiffness due to bond slip, shear cracks, and energy absorption characteristics of the structure during an earthquake excitation. The stiffness of Takeda's model during unloading (K_r) was defined by Eq. (1).

$$K_r = (M_c + M_y) / (\theta_c + \theta_y) \left| \theta_y / \theta_m \right|^{\alpha} \quad (1)$$

where α was the unloading stiffness parameter that was considered equal to 0.4 for the RC columns. The earthquake excitation during the sub-structured pseudo-dynamic test was the modified Hyogo-Ken Nanbu 1995 earthquake excitation (NS direction). The Hyogo-ken Nanbu earthquake excitation was selected to represent a near field excitation. The time scale was amplified to half the original time scale that was recorded during the original Hyogo-Ken Nanbu excitation. The maximum ground acceleration that was considered during the sub-structured pseudo-dynamic test was kept as the original acceleration (818 gal) that was recorded during the original excitation [15], [16] (Fig. 4c).

The so-called mixed (explicit-implicit) integration method that was originally developed for finite elements analysis was found to be suitable for the sub-structured pseudo-dynamic test [10]. However, Nakashima et al. [17] found out that for the sub-structured pseudo-dynamic test, the constitutive Operator Splitting (OS) method is the most effective method in terms of both stability and accuracy. Consequently, the OS method was implemented in this study for the numerical integration of the equation of motion. The integration time interval was 0.0005 second and the earthquake time interval was 0.005 second.

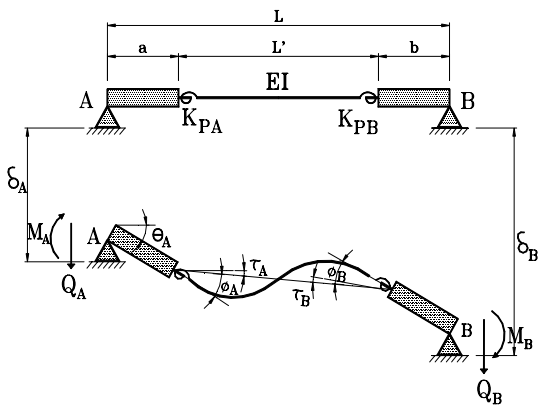

a) One component model

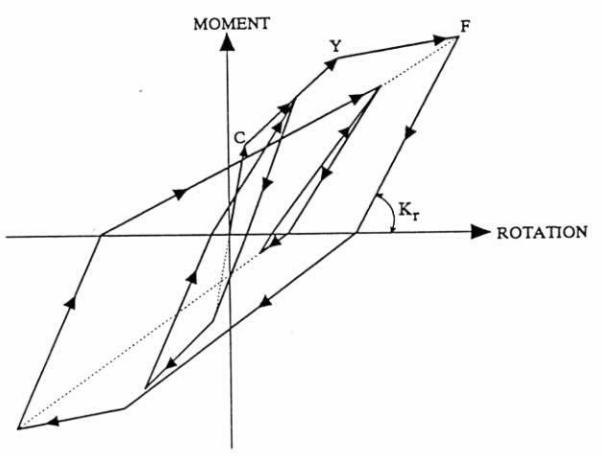

b) Takeda's hysteretic restoring force model

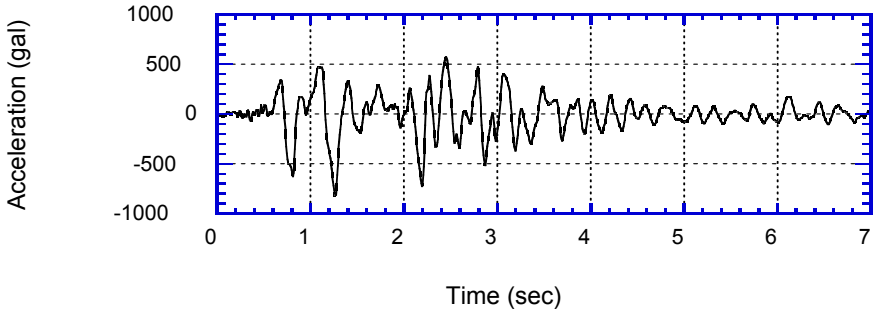

c) Input ground excitation (Hyogo-Ken Nanbu Earthquake, 1995, Kobe city, NS direction)

Fig. 4 One Component Model, Takeda's Tri-Linear Hysteretic Restoring Force Model, and Input Ground Acceleration

Two percent damping was assumed for each mode of the modal damping until the member under consideration experience a rotation angle equal to the yield rotation angle. After reaching the yield rotation angle, the damping was assumed to become zero due to the fact that only the hysteretic damping is dominant after the displacement reaches the yield displacement. The system that was used in the sub-structured pseudo-dynamic test consists of the specimen, loading actuator, reaction wall, data loggers, personal computer for analyzing the inelastic response of the viaduct model and for controlling the input/output data, measuring devices, another personal computer for data acquisition, digital/analog (*D/A)* converter, and analog/ digital *(A/D)* converter. The test procedures were as follows:

1) The displacement of the girder at the first step was calculated analytically by the response analysis program that was based on Takeda's tri-linear model.
2) By means of the digital/analog converter, the calculated displacement was converted from a digital value into an analog value that can be applied to the specimen through the actuator.
3) Immediately after the actuator applies the required displacement to the specimen, the restoring force was directly measured from the loading system. The computer records this restoring force after converting the data from analog to digital through the *A/D* converter.
4) The previous restoring force was used for the calculation of the displacement in the next step.
5) The previous steps (step 1-4) were repeated for the entire duration of the input excitation.

TEST RESULTS

STATICALLY REVERSED CYCLIC LOADING TEST RESULTS

The input cyclic wave, shown in Fig. 3, was employed during the statically reversed cyclic loading testing of specimen B-1. Fig. 5a shows the load-displacement curve for specimen B-1. The test was continued, after reaching the ultimate load, till a decrease of the load to 80 percent of the ultimate load was noticed. The 80 percent is a common acceptance criterion stipulated in the New Zealand standards [18], and has been adopted by many prominent researchers [1].

The maximum displacement, in the two directions of loading was about 5 times the yielding displacement of the prestressing tendons. The skeleton (backbone) curve for the specimen was experimentally obtained and shown in Fig. 5b. The anticipated bond-slip of the reinforcement and prestressing tendons was considered while predicting the analytical skeleton curve. A good agreement between the analytical and the experimental skeleton curves was found (Fig. 5b).

The flexural cracks were opened and closed while almost no shear cracks were observed during the test. The hysteretic loops shown in Fig. 5a shows stiffness degradation and a change in stiffness during reloading which is known as pinching [19]. The pinching can be

attributed to opening and closing of the cracks during the cyclic loading. Shear, which is generally responsible for the pinching of the load-deformation curve, was not the cause of the pinching.

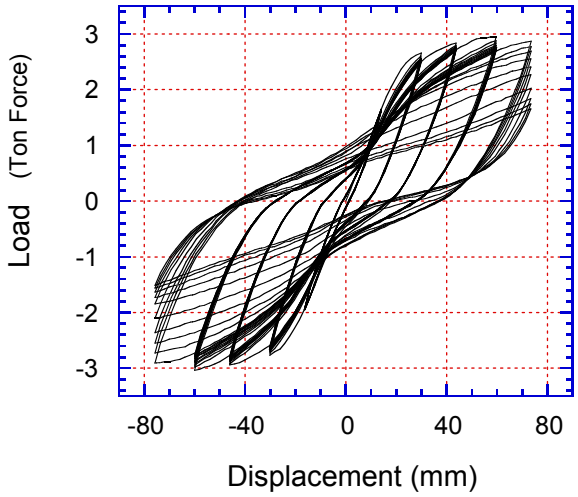

a) Hysteretic load-displacement curve

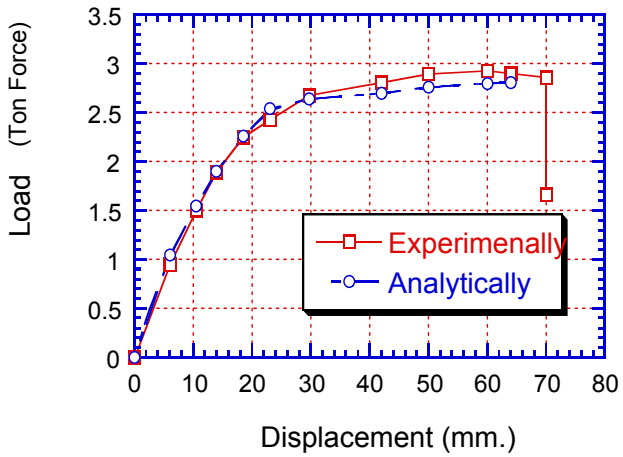

b) Experimental and analytical back-bone curves

Fig. 5 Hysteretic Load-Displacement and Back-Bone Curves for Specimen B-1 during the Statically Reversed Cyclic Loading Test

Specimen B-1 was a partially prestressed concrete specimen, and therefore the pinching was not significant. Consequently, a higher energy dissipation capacity than that a fully prestressed concrete member was attained. The hysteretic load-displacement curve (Fig. 5a) shows a stable behavior with a comparatively minor strength enhancement.

At early stages of loading, and until a displacement of three times the yield displacement of the PC tendons, the residual tensile forces in the PC tendons were adequate to close previously opened cracks. At a displacement equals to 4 times the yielding displacement of the PC tendon, the concrete compression strains in the plastic hinge region exceeded the unconfined compression strain capacity and concrete cover spalling was noticeable. Because of the existence of relatively close-spaced transverse hoops, crushing was delayed inside the concrete core as they act to restrain the lateral compression of the concrete that accompanies the onset of crushing, thus maintaining the integrity of the concrete core. It was not until a displacement of five times the yield displacement when the crushing began to penetrate inside the core concrete due to the large number of repetitions of the cycles. Additionally, the reinforcing bars experienced large increase in the tensile strains and buckling after cover spalling in the plastic hinge region. The cracking pattern of specimen B-1 after the test is shown in Fig. 6.

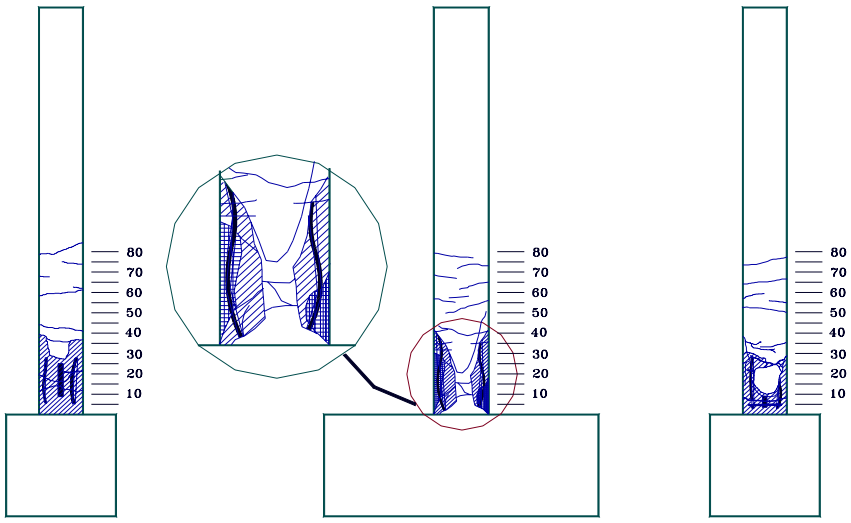

Heights are given in cm.

Fig. 6 Cracking Pattern of Specimen B-1 at the End of the Statically Reversed Cyclic Loading Test

SUB-STRUCTURED PSEUDO-DYNAMIC TEST RESULTS

The used time history of the actuator load during the test is shown in Fig. 7a. The resulting hysteretic moment-rotation curve for the left end of the PC girder is shown in Fig. 7b. Pinching of the hysteretic loops is clear in Fig. 7b. A maximum rotation angle of 0.045 rad. was observed and the Fig. also indicates a considerable damage of the PC girder due to the input excitation.

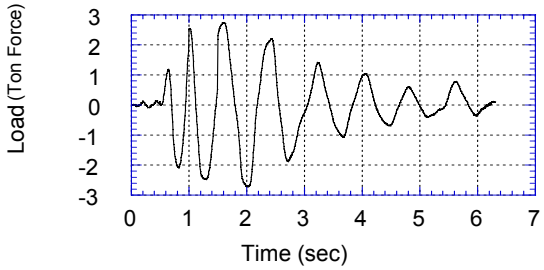

a) Load-time history of the actuator

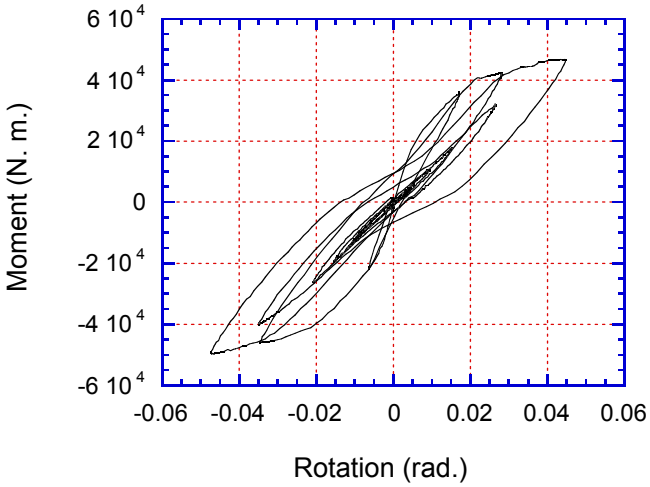

b) Experimental hysteretic moment rotation curve for the left end of the PC girder

Fig. 7 Load-Time History of the Actuator and Experimental Hysteretic Moment-Rotation Curve for the Left End of the PC Girder

Fig. 8a shows the hysteretic moment-rotation curve of the bottom end of the left column of the viaduct model. It can be noticed from the curve that considerable damage occurred during the input excitation. A maximum rotation of 0.036 rad. was observed. Fig. 8b shows the hysteretic moment-curvature curve of the top end of the left column of the viaduct model. It can be observed from the curve that limited energy was dissipated in the plastic hinge that was expected to form at the top of the left column of the viaduct model. Similar results were obtained for the bottom and top ends of the right column of the viaduct model. A comparison between the hysteretic moment-rotation curves in Fig. 7b and Fig. 8a shows that not only the reinforced concrete column but also the PC girder may undergo extensive damage during an earthquake excitation. As a consequence, adequate care should be given to the PC girder design to satisfy the requirements of a seismic resistant structure.

The time history of the response acceleration (Fig. 9a) shows that the maximum observed acceleration was 12.2 m/sec^2 that occurred at a time equal to 1.25 second. The time and direction of the maximum acceleration were consistent with the time and direction of the maximum input ground acceleration (Fig. 4c). The time history of the response displacement (Fig. 9b) shows that the maximum displacement was 8.5 cm, which occurred at a time equal to 1.95 second.

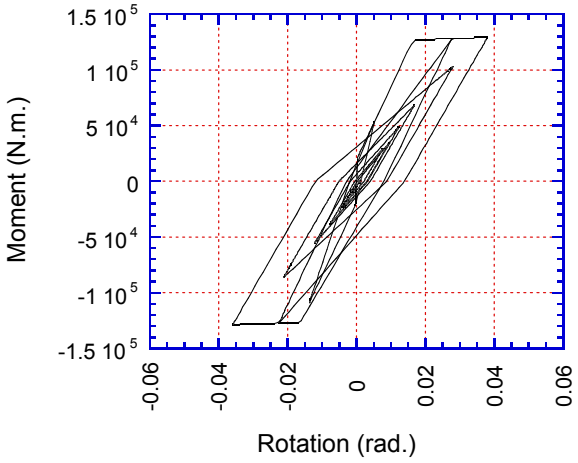

a) Experimental hysteretic moment rotation curve for the bottom end of the RC columns

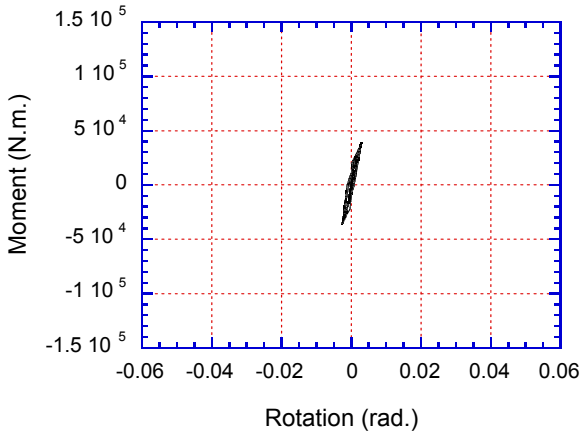

b) Experimental hysteretic moment rotation curve for the top end of the RC columns

Fig. 8 Experimental Hysteretic Moment-Rotation Curves of the Bottom and Top Ends for the RC Columns during the Sub-Structured Pseudo-Dynamic Testing

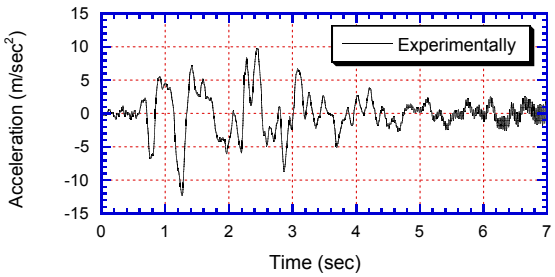

a) Acceleration-time history

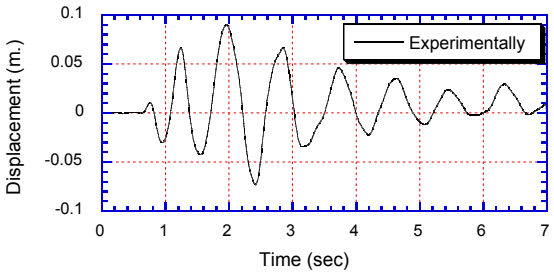

b) displacement-time history

Fig. 9 Experimental Acceleration-Time History and Displacement-Time History during the Sub-Structured Pseudo-Dynamic Testing

RESPONSE ANALYSES OF THE EXPERIMENTAL VIADUCT MODEL

The results that were obtained from the reversed cyclic loading tests and the sub-structured pseudo-dynamic tests for the tested viaduct models shows that not only the RC columns but also the PC girders may be damaged during earthquake excitations. This conclusion can not be generalized without investigating to what extent changes in the viaduct model can influence the resulting response behavior and ductility factor. A parametric study that includes parameters such as the yielding ratio (P_y/mg), the elastic natural period, and the strength ratio between the PC girder and the RC columns can verify the above conclusion.

The accuracy of any parametric study is dependent on the accuracy of the available analytical hysteretic restoring force models for prestressed and reinforced concrete members of the viaduct model. Therefore, response analyses were carried out for the same viaduct model that was tested using the sub-structured pseudo-dynamic test in the previous section. The response analyses results were compared with the experimental results of the sub-structured pseudo-dynamic test.

One component model, which was proposed by Giberson [11], was employed during the response analyses. Takeda's tri-linear restoring force model was used for the RC columns and the modified Takeda's model was used for the PC girders. The modified Takeda's model [7] accounts for the partial prestressing that was applied to the girders. Zatar et al. [20] and [21] presented and verified the accuracy of another restoring force model for prestressed and partially prestressed members. The model by Zatar et al. incorporated modifications for Takeda's restoring force model.

Fig. 10a shows the hysteretic moment-rotation curve analytically obtained for the left end of the PC girder. The maximum moment was $-5.15*10^{-4}$ N.m and the corresponding rotation was -0.043 rad.

Fig. 10b and Fig. 10c show the hysteretic moment-rotation curves for the bottom and the top ends of the RC column, respectively. Little energy was dissipated at the top end of the column. Conversely, considerable damage was observed at the plastic hinge that existed at the bottom end of the RC column. The maximum moment in the bottom end of the column was $1.3*10^{5}$ N.m and the corresponding rotation was -0.042 rad.

A comparison was made between the experimental and analytical hysteretic moment-rotation curves for the left end of the PC girder and for the bottom and the top ends of the RC column, respectively (Fig. 7, 8, and 10). The comparison included the observed damage, the hysteretic behavior, the maximum moment, and the associated rotation. An overall good agreement was found between the sub-structured pseudo-dynamic test and the response analyses results. The unloading stiffness of the hysteretic moment-rotation curve of the PC girder that was obtained from the response analyses was different from the unloading stiffness that was found during the sub-structured pseudo-dynamic test. However, the total dissipated energy that was obtained from the response analyses was found to be almost similar to the experimentally dissipated energy during the excitation.

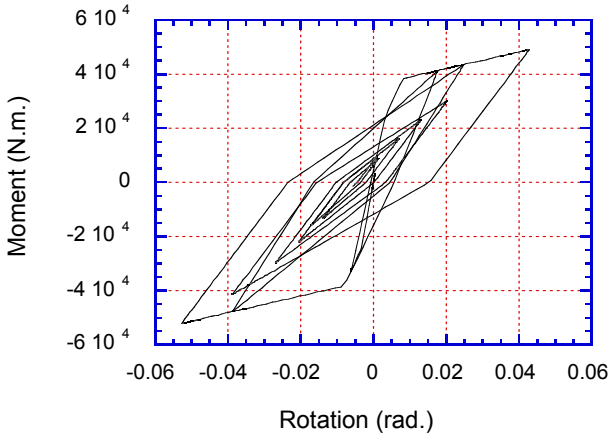

a) Analytical moment-rotation curve for the left end of the PC girder

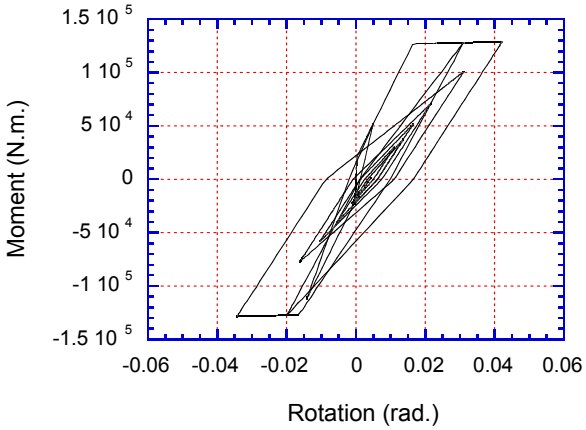

b) Analytical moment-rotation curve for the bottom end of the RC columns

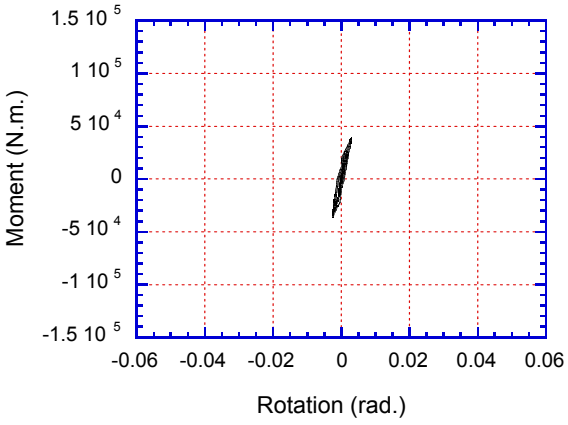

c) Analytical moment-rotation curve for the top end of the RC columns

Fig. 10 Analytical Hysteretic Moment-Rotation Curves of the Left End for the PC Girder and the Bottom and Top Ends of the RC Columns

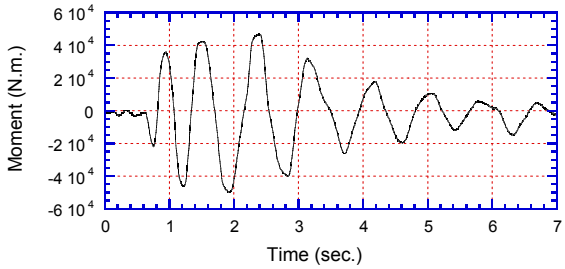

a) Experimental moment-time history for the left end of the PC girder

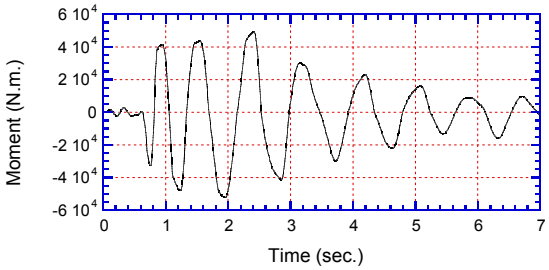

b) Analytical moment-time history for the left end of the PC girder

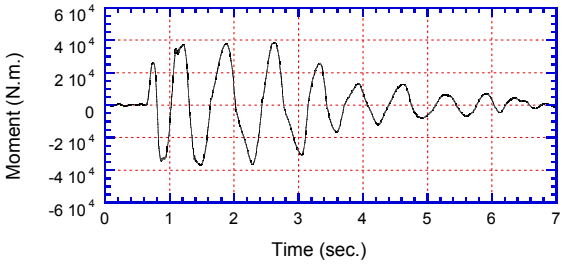

c) Experimental moment-time history for the top end of the RC columns

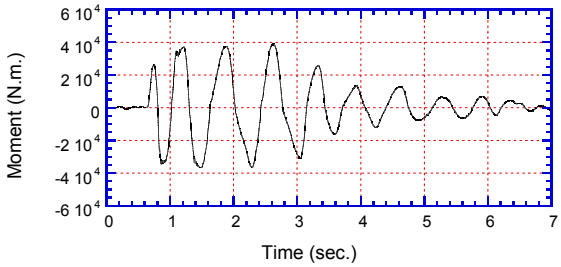

d) Analytical moment-time history for the top end of the RC columns

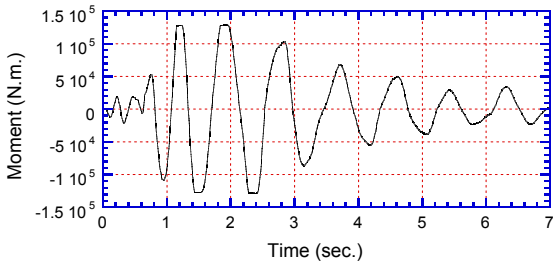

e) Experimental moment-time history for the bottom end of the RC columns

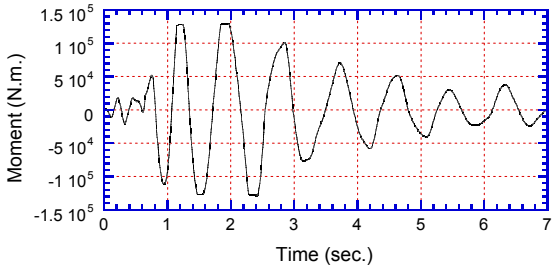

f) Analytical moment-time history for the bottom end of the RC columns

Fig. 11 Experimental Versus Analytical Moment-Time History for the Left End of the PC Girder and the Top and Bottom Ends of the RC Columns

The moment-time history curves that were obtained from the sub-structured pseudo-dynamic test for the left end of the PC girder and the bottom and the top ends of the RC column are shown in Fig. 11a, Fig. 11c, and Fig. 11e, respectively. The corresponding moment-time history curves that were obtained from the response analyses are shown in Fig. 11b, Fig. 11d, and Fig. 11f, respectively. The comparison between the experimental and analytical moment time-histories shows good agreement, thus verifying the accuracy of the used analytical hysteretic restoring force models for both the prestressed and the reinforced concrete members of the viaduct model.

PARAMETRIC STUDY OF THE VIADUCT MODELS

The statically reversed cyclic loading and sub-structured pseudo-dynamic testing clarified that not only the RC columns but also the PC girders can have some seismic damage during earthquake excitations. It was also shown that because of the common use of un-symmetric PC girder cross sections, one direction might not be capable of sustaining the imposed loads resulting from the excitation. These findings were based on certain characteristics of the cross sections of both the RC piers and the PC girders. Consequently, the objective of this part of study is to conduct a parametric study that clarifies the influence of some parameters on the resulting response and ductility factor. The parametric study includes the yielding ratio (P_y/mg), elastic natural period, relative strength between the PC girder and the RC pier and the relative strength between bottom and top sides of the PC girder.

Three-spanned viaduct models, which have similar span length to that of the sub-structured pseudo-dynamic test specimen, were employed. Cross-sectional dimensions of the RC piers are the same for all models (25 cm x 40 cm). The reinforcement details of the RC piers are shown in Fig. 12. In order to obtain different relative strength between the PC girders and the RC piers, ten cases were considered. The cross sections of the PC girders vary as shown in Table 1. The strength ratios range from 0.2 to 1.0. Prestressed concrete girder cross section of 20 cm x 25 cm was used. Nine types named A-1 up to A-9 were used in which the relative capacity between the top and bottom sides of the PC girders ranges from 0.25 to 1.0 (Table 2). The longitudinal reinforcement in the RC pier was changed to study the influence of the yielding ratio (P_y/mg) on the resulting ductility factor. The yielding ratio ranges from 0.2 to 0.7 (Table 3). Inelastic response analyses were carried out using the restoring force model that is shown in the last section (Response Analyses Results). One component model was considered. The Hyogo-Ken Nanbu 1995 earthquake excitation 1995 (N-S directions) with a maximum acceleration of 818 gal was used.

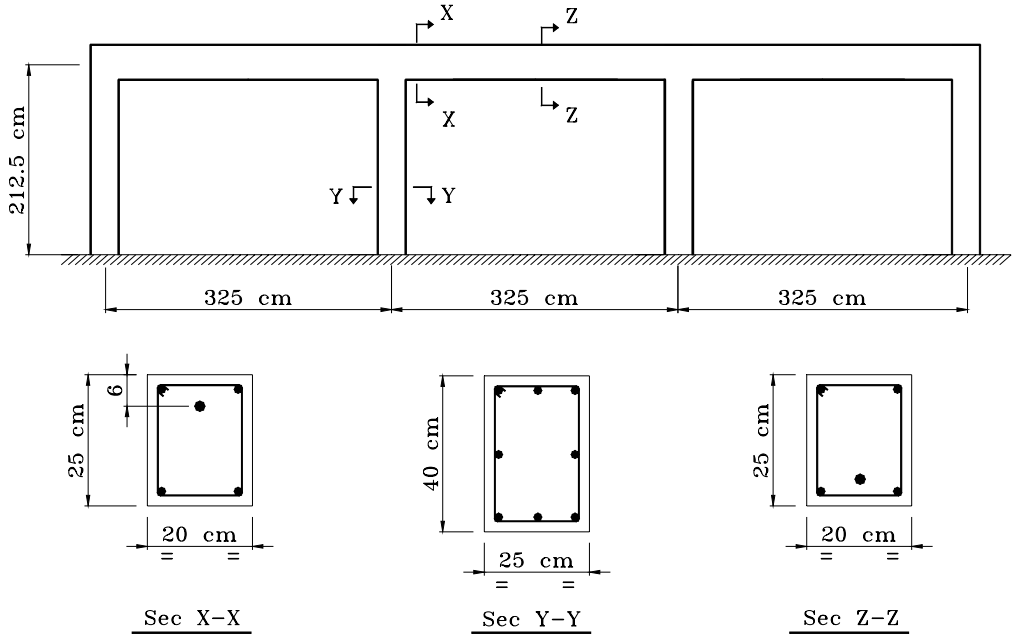

Fig. 12 Dimensions of the Viaduct Model

Table 1 Cross Sections of the Viaduct Model

Case No.	PC girder cross section b*d, *cm*	Yielding capacity of top side of PC girder, *kN.m*	Yielding capacity of bottom side of PC girder, *kN.m*	Capacity ratio = ratio of top side capacity of PC girder / capacity of RC pier
Case 1	20*20	24	6	0.2
Case 2	20*22.5	30	7	0.25
Case 3	20*25	36	10	0.3
Case 4	22.5*27.5	48	12.5	0.4
Case 5	25*27.5	60	14	0.5
Case 6	25*30	71	15	0.6
Case 7	27.5*30	84	16.5	0.7
Case 8	27.5*32.5	97	17.5	0.81
Case 9	30*32.5	110	19	0.92
Case 10	30*35	120	20	1

Table 2 Characteristics of the PC Girders with Un-symmetric Cross Sections

Case No.	Yielding moment of top side of PC girder, *kN.m*	Yielding moment of bottom side of PC girder, *kN.m*	PC girder capacity ratio = ratio of bottom side capacity / top side capacity of PC girder
A-1	36	9	0.25
A-2	36	10.8	0.3
A-3	36	13.7	0.38
A-4	36	18	0.5
A-5	36	22.7	0.63
A-6	36	25.2	0.7
A-7	36	27	0.75
A-8	36	31.7	0.88
A-9	36	36	1

Table 3 Cross Sections of the RC Piers

Yielding ratio of RC pier $= P_y / mg$	Main Reinforcement ratio of RC pier (%)	Yielding capacity of RC pier, *kN.m*	Capacity ratio = ratio of of top side capacity of PC girder / capacity of RC pier
0.2	1	60	0.7
0.3	2.1	90	0.5
0.4	2.9	120	0.4
0.5	3.8	150	0.3
0.6	4.4	180	0.25
0.7	5.1	210	0.2

Results were obtained for each case of the parametric study in terms of hysteretic moment-rotation curves and time histories of displacement, velocity and acceleration. Ductility factor for each member in all cases was obtained at both ends of each member. As a result of the commonly used un-symmetric arrangement of prestressing tendons and reinforcing bars in the PC girders, the flexural capacity differed thus changing the ductility factors at both the top and bottom sides of the PC girders. Because of space limitations, only the resulting ductility factor for the inner PC girder and RC pier will be shown. Results obtained for the expected plastic hinges at the top and bottom ends of the RC pier and for the left end of the PC girder are presented.

Fig. 13 shows the influence of the capacity ratio between the top side of the PC girder and the RC pier on the resulting ductility factor for a viaduct model with an un-symmetric PC girder that has a certain relative capacity between both sides of the girder. It can be observed that increasing the capacity ratio between the PC girders and the RC piers results in a reduced ductility factor in the bottom side of the plastic hinges, which were formed at the end of the PC girder. The plastic hinge at the end of the PC girder experienced significant ductility factors in the bottom side as a result of its reduced capacity as compared to the ductility factors obtained for the plastic hinges formed at the top and bottom ends of the RC pier or as compared to the top side of the PC girder. The increased capacity ratio results in decreasing the ductility factor of the plastic at the bottom end of the RC pier and the top side of the PC girder. On the other hand, the ductility factor at the top end of the RC pier increases by increasing the capacity ratio.

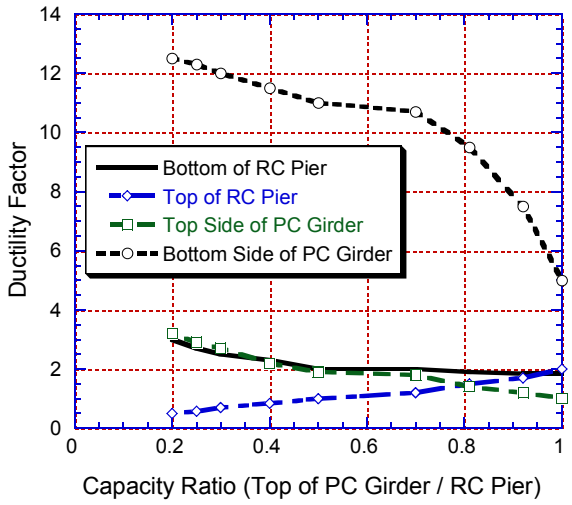

Fig. 13 Capacity Ratio versus Ductility Factor for the Viaduct Models with Un-Symmetric Girders

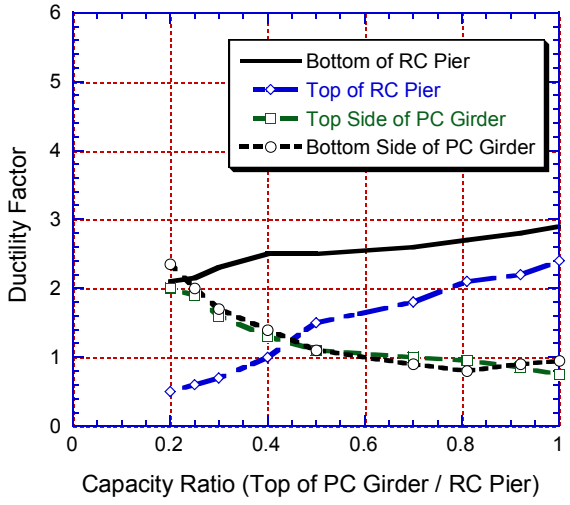

Fig. 14 Capacity Ratio versus Ductility Factor for the Viaduct Models with Symmetric Girders

Fig. 14 shows the influence of the capacity ratio between the top side of the PC girder and the RC pier on the resulting ductility factor for the viaduct model. The values shown in Fig. 14 are based on assuming that the PC girder has a symmetric capacity at both the top and bottom sides. A comparison between the case of un-symmetric and symmetric PC girders in

Fig. 13 and Fig. 14 shows that the use of symmetric girder can significantly result in decreasing the obtained ductility factor at the bottom side of the PC girder. Fig. 14 also shows that increasing the capacity ratio between the PC girder and the RC pier results in increasing the obtained ductility factor in the plastic hinges formed at the top and bottom ends of the RC pier. On the contrary, the resulted ductility factor decreases for both the top and bottom sides in the plastic hinge formed at the end of the PC girder as a result of increasing the capacity ratio.

Fig. 15 shows the influence of changing the PC girder capacity on the resulting ductility factor for both the PC girder and the RC pier. The PC girder capacity ratio is defined herein as the ratio between the yielding capacity of the bottom side and the yielding capacity at the top side of such PC girder. The PC girder dimensions are according to case 3 (Table 1) where the capacity ratio equals to 0.3. Fig. 15 shows that the ductility factor for the bottom side of the PC girder is the highest among the others. The difference between the ductility factor for the bottom side and the others reduces as a result of increasing the PC girder capacity ratio. The observed ductility factors of the symmetric PC girder at both sides for are identical and of a small value as compared to that at the bottom side of the PC girder when the corresponding PC girder capacity ratio is small. Fig. 15 also implies that the top end of the RC pier did not experience yielding for all PC girder capacity ratios. The ductility factors for the plastic hinges at the bottom end of the RC pier and the top side of the PC girder did not experience much difference by increasing the PC girder capacity ratio.

Fig. 16 shows that the influence of the relative PC girder capacity ratio on the resulting ductility factors for case 6 in Table 1, where an increased PC cross section of 25 x 30 cm, resulted in capacity ratio of 0.6. The figure implies almost the same observations from Fig. 15 with the exception that the influence of increasing the PC girder capacity can further decrease the observed ductility factor in the bottom side of the PC girder. A similar observation can be noticed for the top side of the PC girder. On the contrary, the ductility factor for the bottom end of the RC pier tends to increase by increasing the PC girder capacity ratio.

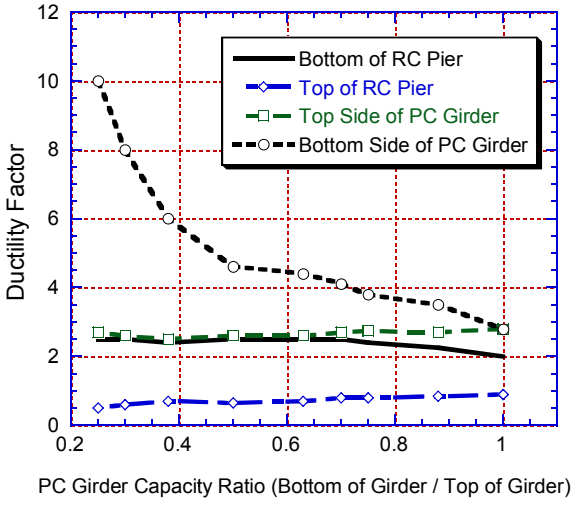

Fig. 15 PC Girder Capacity Ratio versus Ductility Factor for Viaduct Model Case 3

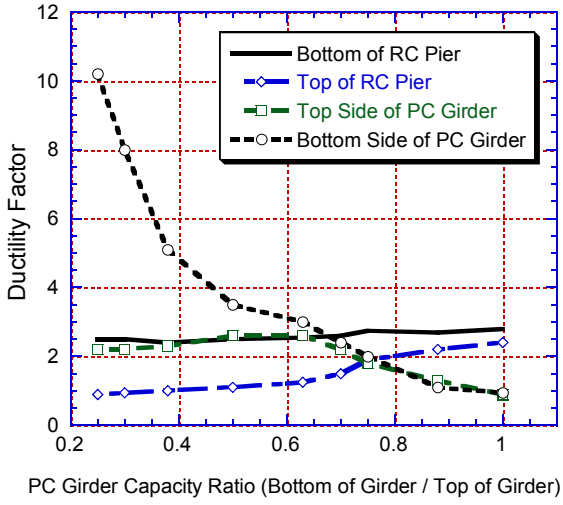

Fig. 16 Capacity Ratio versus Ductility Factor for Viaduct Model Case 6

Fig. 17 shows the influence of the yielding ratio (P_y/mg) of the RC pier on the resulting ductility factor. The considered yielding capacities of the RC pier and the associated yielding ratios are given in Table 3. It can be observed that increasing the yielding ratio of RC pier results in slight increase in the resulting ductility factor at the bottom side of the plastic hinge of the PC girder. Although the obtained ductility factors for the top side of the PC girder were much smaller than those in the bottom side of the PC girder, a similar observation was also found for the top side of the PC girder. The plastic hinges at the bottom end of the RC pier experienced higher ductility factors than those for the top end of the pier.

Fig. 18 shows the influence of changing the elastic natural period of the viaduct model on the resulting ductility factors of both the RC pier and the PC girder. Increasing the natural period resulted from increasing the heights of the RC pier. The natural periods of the viaduct models range from 0.2 sec to 0.75 sec. The highest observed ductility factors were those of the bottom side of the PC girder. The increased elastic natural period results in subsequent decrease in the ductility factors of all plastic hinges in both the RC pier and the PC girder especially for the bottom side of the PC girder It was concluded that the larger the natural period of the viaduct structure, the lower the resulting response for all members of the viaduct structure, including the critical bottom side of the un-symmetric PC girder. Therefore, it is recommended that the viaduct structures be designed to possess natural periods exceeding 0.6 seconds.

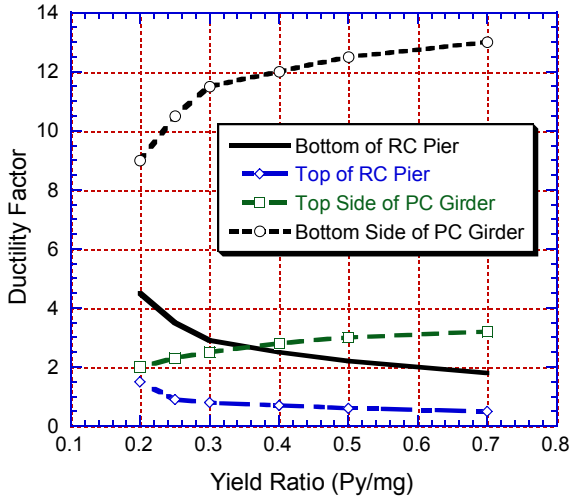

Fig. 17 Yielding Ratio versus Ductility Factor for the Viaduct Models

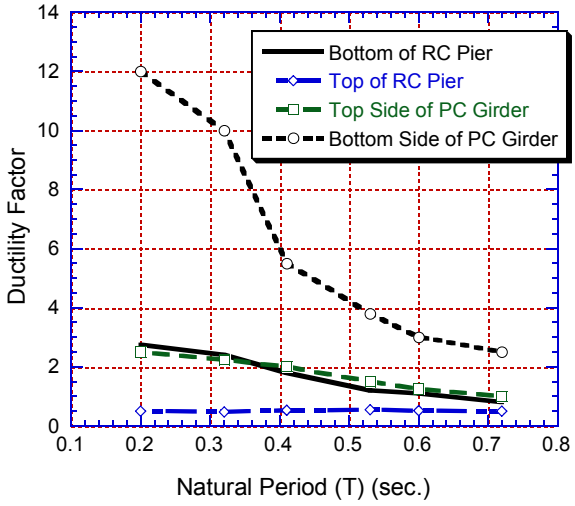

Fig. 18 Natural Period versus Ductility Factor for the Viaduct Models

CONCLUSIONS

The objective of this study was to assess the dynamic behavior of monolithic prestressed concrete highway viaduct structures. The study included experimental and analytical phases. Small-scaled models were employed so as to represent actual viaduct structures. Specimens

representing PC girders of the viaducts were tested experimentally. Two testing techniques were employed in the experimental phase of the study. The first technique was a statically reversed cyclic loading test. The objective of the statically reversed cyclic loading test was to study the inelastic response behavior of the PC girders and to obtain the hysteretic-load deformational characteristics. The sub-structured pseudo-dynamic testing scheme was implemented as the second testing technique. During the sub-structured pseudo-dynamic test, the PC girder was tested experimentally and the RC columns of the viaduct structure were simulated analytically. Response analyses for the same viaduct model, in terms of hysteretic moment-rotation curves and time-histories, were carried out. From the test results, it was concluded that:

1) Not only the RC columns but also the PC girders are subjected to inelastic deformations that may cause a considerable damage during earthquake excitations. As a consequence, adequate care should be given to the PC girder design to satisfy the strength and ductility requirements of seismic resistant structures.
2) A comparison between the experimental and analytical results in terms of the resulting skeleton curves, time histories, hysteretic curves, and the dissipated energy was made. A good agreement between the experimental and analytical results was found. The analytical model's applicability was verified for further utilization in parametric studies that aim at clarifying the response behavior of prestressed concrete viaduct structures.

A parametric study that was based on the calibrated hysteretic restoring force model is carried out. The study included parameters such as the yielding ratio (P_y/mg), elastic natural period, strength ratio between the PC girder and the RC pier, and strength ratio between the bottom and top sides of the PC girder. Three-span models were considered in the study. The difference between utilizing symmetric and un-symmetric PC girders on the resulting ductility factor was clarified. The parametric study revealed that the larger the PC girder capacity the smaller the observed ductility factor in the bottom side of the PC girder. The ductility factors for the plastic hinges at the bottom end of the RC pier and the top side of the PC girder did not experience much difference by increasing the PC girder capacity ratio. The plastic hinge at the bottom end of the RC pier experienced a higher ductility factor than that for the top end of the pier. It was concluded that the larger the natural period of the viaduct structure, the lower the resulting response for all members of the viaduct structure, including the critical bottom side of the un-symmetric PC girder. Therefore, it is recommended that the viaduct structures be designed to possess natural periods exceeding 0.6 seconds. The higher the yielding ratio for the RC piers of the viaduct structures the lower the dynamic response of the viaduct structure. The study shall assist bridge engineers designing reliable viaduct structure in areas with a considerable seismic risk. The results of the parametric study shall assist developing seismic design guidelines for monolithic prestressed concrete highway viaduct structures.

ACKNOWLEDGMENT

The author would also like to acknowledge the members of the structural laboratory at Saitama University who provided assistance during the experimental phase of the study. The

author would like to acknowledge Dr. Hiroshi Mutsuyoshi, a structural engineering professor at Saitama University, for his valued assistance, full support, and appreciated comments. Additionally, the financial support of the Grant-in-aid of the Ministry of Education, Science and Culture in Japan is greatly appreciated.

REFERENCES

1) Priestley, M. J. N., F. Seible, and G. M. Calvi. *Seismic Design and Retrofit of Bridges.* John Wiley & Sons Inc., New York, 1996.
2) Harajli, M. and Naaman, A.E. Deformation and Cracking of Partially Prestressed Concrete Beams under Static and Cyclic Fatigue Loading. *Report No. UMEE 84R1,* Department of Civil Engineering, the University of Michigan College of Engineering, Ann Arbor, Michigan, August 1984.
3) Zatar, W. and H. Mutsuyoshi. Residual Displacements of Concrete Bridge Piers Subjected to Near Field Earthquakes. *American Concrete Institute Structural Journal*, Title No.99-S74, Vol.99, No.6, Nov./Dec. 2002, pp.740-749.
4) Zatar, W., H. Mutsuyoshi, and H. Koizumi. A Restoring Force Model for Partially Prestressed Concrete. *Transactions of the Japan Concrete Institute*, Vol. 21, 1999, pp.247-254.
5) Zatar, W. and H. Mutsuyoshi. Earthquake Damage of Prestressed Concrete Viaduct Structures. *International Association of Bridge and Structural Engineering (IABSE) Symposium of Long-Span and High-Rise Buildings*, Sep. 1998.
6) Zatar, W. and H. Mutsuyoshi. Dynamic Response Behavior of Prestressed Concrete Viaduct under Severe Earthquake. *Proceedings of the Workshop on Earthquake Engineering Frontiers in Transportation Facilities*, Technical Report *NCEER*-97-0005, 1997.
7) Hosaka, I., H. Mutsuyoshi, W. Zatar, and W. Tanzo. Behavior of Concrete Viaduct Structures. *Transactions of the Japan Concrete Institute*, Vol. 19, 1997, pp.171-177.
8) Yamada, Y., H., Iemura, and W. Tanzo. Sub-structured Hybrid Loading of Structural Members under Combined Axial, Shear, and Bending Loads. *8th Symposium of Earthquake Mechanics* in Japan, 1990, pp.1503-1508.
9) Mutsuyoshi, H., A. Machida, K. Sadasue, and S. Oba. Earthquake Response Behavior of First-Level Girder in R/C Frame Structure Based on Pseudo-Dynamic Test Method. *Transactions of the Japan Concrete Institute*, Vol. 14, 1992, pp.289-296.
10) Mutsuyoshi, H., W. Tanzo, and A. Machida. Influence of Member Ductility on The Total Seismic Response of RC Piers Using Sub-structured Pseudo-Dynamic Tests. *Transactions of the Japan Concrete Institute*, Vol. 15, 1993, pp.353-360.
11) Giberson, M. F. Two Nonlinear Beams with Definitions of Ductility. *American Society of Civil Engineers Structural Journal*, Vol. 95, No. ST2, 1969.
12) Otani, S. Inelastic Analysis of R/C Frame Structures. *American Society of Civil Engineers Structural Journal*, Vol. 100, No. ST2, 1974.

13) Ohta, M. A Study on Earthquake Resistant Design for Reinforced Concrete Bridge Piers of Single Column Type. *Report of the Ministry of Construction*, Japan, Vol. 153, 1980.

14) Takeda, T., M. A. Sozen, and N. N. Nielsen. Reinforced Concrete Response to Simulated Earthquake. *American Society of Civil Engineers Structural Journal*, Vol. 96, No. ST2, paper 7759, Dec., 1970, pp.2557-2573.

15) Preliminary Report on the Great Hansion Earthquake, January 17, *Proceedings of the Japan Society of Civil Engineers,* 1995.

16) Ghasemi, H., Otsuka, H., Cooper, J.D., and Nakajima, H., Report on the Aftermath of the Kobe Earthquake, *United States Department of Transportation-Federal Highway Administration,* TFHRC, Fall 1996, Vol. 60, No. 2.

17) Nakashima, Ishida, and Ando. Numerical Integration Methods for Substructure Pseudo-Dynamic Test Method. *Transactions of the Architectural Institute of Japan*, Structural Engineering Series, No. 417, 1990, pp.107-117. (In Japanese)

18) NZS 4203. New Zealand Standard, Code of Practice for General Structural Design and Design Loadings for Buildings, *Standard Association of New Zealand*, 1976, pp.80.

19) Saatcioglu, M. Modeling Hysteretic Force-Deformation Relationship for Reinforced Concrete Elements, Earthquake Resistant Concrete Structures, Inelastic Response and Design, *American Concrete Institute Special Publication, ACI SP-127-5*, 1991, pp.153-198.

20) Zatar, W. and H. Mutsuyoshi. Logical On-line Hybrid Computer Actuator and Quasi-static Testing Schemes of PC Columns. *International Journal of Information Technology in Architecture, Engineering and Construction*, Mill press, Vol. 1, Issue 3, Sep. 2003, pp.209-224.

21) Zatar, W. and H. Mutsuyoshi. Control of Residual Displacements of RC Piers by Prestressing. *American Society of Civil Engineers (ASCE) Publication*, ISBN 0-7844-0553-0, Library of Congress Catalog Card No. 2001-018922, 2001.

22) Zatar, W. Seismic Behavior of Prestressed Concrete Bridge Piers and Viaducts. D. Eng. Dissertation, Department of Civil and Environmental Engineering, Saitama University, Japan, 1999.